Fine-Grained Localization for Multiple Transceiver-Free Objects by using RF-Based Technologies

Dian Zhang, *Member, IEEE*, Kezhong Lu, *Member, IEEE*, Rui Mao, *Member, IEEE*, Yuhong Feng, Yunhuai Liu, *Member, IEEE*, Zhong Ming, and Lionel M. Ni, *Fellow, IEEE*

Abstract—In traditional radio-based localization methods, the target object has to carry a transmitter (e.g., active RFID), a receiver (e.g., 802.11× detector), or a transceiver (e.g., sensor node). However, in some applications, such as safe guard systems, it is not possible to meet this precondition. In this paper, we propose a model of signal dynamics to allow the tracking of a transceiver-free object. Based on radio signal strength indicator (RSSI), which is readily available in wireless communication, three centralized tracking algorithms, and one distributed tracking algorithm are proposed to eliminate noise behaviors and improve accuracy. The midpoint and intersection algorithms can be applied to track a single object without calibration, while the best-cover algorithm has higher tracking accuracy but requires calibration. The probabilistic cover algorithm is based on distributed dynamic clustering. It can dramatically improve the localization accuracy when multiple objects are present. Our experimental test-bed is a grid sensor array based on MICA2 sensor nodes. The experimental results show that the localization accuracy for single object can reach about 0.8 m and for multiple objects is about 1 m.

Index Terms—Applications, pervasive computing, tracking, wireless sensor networks, multiple transceiver-free objects

1 Introduction

Real-time tracking of moving objects is highly in demand and important to many applications, such as vehicle tracking [5], animal habitat monitoring [21]. It has attracted a great deal of attention in various research communities. GPS [17] is a technology well known for its accuracy. However, GPS only works in outdoor environments without satellite signals being blocked. Moving object tracking in indoor environments is more complicated and several technologies, such as video, pressure, infrared, have been proposed. These technologies are usually costly, including infrastructure, deployment, and maintenance, and may have some restrictions placed on the environments in which they are applied. For example, video technology based on real-time image processing is a feasible solution. However, video technology does not work in dark environments and the privacy of those being tracked creates another concern.

Radio frequency (RF) is another promising technology, which utilizes *Radio Signal Strength Indicator* (RSSI) to track moving objects if both moving objects and some reference objects are using RF signals to communicate. In theory, the RSSI obtained by the receiver is a function of the distance between the transmitter and the receiver as indicated in many propagation models [14]. However, in practice, there are many problems in applying these models. The indoor layout structure, objects, and humans can cause reflection, refraction, diffraction, and absorption of radio signals. Therefore, severe multi-path phenomenon will occur and affect the accuracy of indoor location sensing. Moreover, many other factors also influence the RSSI, such as temperature, orientation of antenna, and height to the ground [1]. Nevertheless, since RSSI is readily available in wireless communication without additional cost, RF-based localization has become a hot research issue in wireless networks [6], [10], [11], [21].

In RF-based localization, both target objects and reference objects have to communicate with others to collect RSSI information for localization. There are three basic models. In the first model, the target has to carry a transmitter (e.g., active RFID tags) to periodically transmit beacon messages (e.g., the ID of the RFID tag). Many receivers (e.g., RFID readers) with known locations may measure the RSSI values of received beacon messages and cooperate to estimate the target locations. In the second model, the target has to carry a receiver (e.g., 802.11× detectors). The target is able to receive RSSI information from nearby transmitters (e.g., 802.11× access points) and estimate its current location. In the third model, each object has a transceiver (e.g., sensor nodes) and exchange information with other objects. Based on the RSSI information collected from nearby objects, the target may be able to estimate its location. To improve the localization accuracy, many techniques have been proposed.

- *D. Zhang is with the College of Computer Science and Software Engineering, Shenzhen University, Guangdong 518060, China. E-mail: serena.dian@gmail.com.*
- *K. Lu, R. Mao, Y. Feng, and Z. Ming are with the College of Computer Science and Software Engineering, Shenzhen University, Guangdong 518060, China. E-mail: {kzlu, mao, yuhongf, mingz}@szu.edu.cn.*
- *Y. Liu is with the Third Research Institute of Ministry of Public Security, Shanghai 2012014, China. E-mail: yunhuai.liu@gmail.com.*
- *L.M. Ni is with the Department of Computer Science and Engineering, Hong Kong University of Science and Technology, Kowloon, Hong Kong. E-mail: ni@cse.ust.hk.*

Manuscript received 30 Nov. 2012; revised 4 Sept. 2013; accepted 13 Sept. 2013. Date of publication 26 Sept. 2013; date of current version 16 May 2014. Recommended for acceptance by J. Cao.
For information on obtaining reprints of this article, please send e-mail to: reprints@ieee.org, and reference the Digital Object Identifier below.
Digital Object Identifier no. 10.1109/TPDS.2013.243

In the above three models, the target has to carry a transmitter, a receiver, or a transceiver. This precondition, however, cannot be met in some applications, such as safe guard systems. The objective of this paper is to investigate if the location of moving objects can be estimated without carrying any RF device in an environment covered by a wireless sensor network (WSN) where sensor nodes exchange information with each other.[1] To the best of our knowledge, we are the first group to propose the idea of tracking both single and multiple transceiver-free objects using RF-technology, and perform a comprehensive study [1], [2] as well. Our initial research shows it is possible using some novel approaches as described later.

The basic idea of this paper is to construct a signal dynamic model to obtain the property of the RSSI changing behaviors in WSNs. Based on this model and its property, we propose three centralized tracking algorithms: midpoint algorithm, intersection algorithm, and best-cover algorithm. The midpoint and intersection algorithms can be applied to track a single object without calibration, while the best-cover algorithm has higher accuracy but requires calibration. For the purpose of tracking multiple objects, we also put forward the probabilistic cover algorithm based on a dynamic clustering, we named *Distributed Dynamic Clustering* (DDC). It is to dynamically form a cluster of those wireless communication nodes whose received signal strengths are influenced by the objects. Dynamic clustering can overcome this problem and construct different clusters according to different objects. By using our model and a probabilistic methodology, we could more easily determine the number of objects in the area and locate them accurately. Moreover, by dynamically adjusting the transmission power when forming clusters, the interference between nodes will be reduced; this can further improve tracking accuracy.

Our experimental test-bed is a grid sensor array based on MICA2 sensor nodes [19] and larger scale test on TelosB sensors [19]. The experimental results show that under the sensor grid setting with side length of 2 m, the tracking accuracy for single object is about 0.8 m and for multiple objects is about 1 m. The tracking latency is only about 2 s. In short, our proposed algorithms can track multiple transceiver-free objects, if they are not crowded in an area covered by a well-structured WSN.

The rest of this paper is organized as follows. In the next section, we provide some related work. Section 3 introduces the signal dynamic model. The tracking algorithms are described in Section 4. We show the experimental results and evaluate the performance in Section 5. Lastly, we conclude the paper and list our future work.

2 Related Work

Other than the RF technology, some other technologies might be used to track moving objects.

2.1 Video

In the computer vision area, by applying many video-based algorithms on sequences of images from a camera or synchronized images captured from multiple cameras, moving people can be tracked [6] or the number of people in a certain area can be counted [18]. However, this technology is expensive and fails in darkness. Moreover, it may violate the privacy of people.

2.2 Laser

Laser ranging [22] is famous for the accuracy of its distance measurement. However, the cost of such technology is usually prohibitive.

2.3 Infrared

In the context of infrared wireless networks, the limited range of an infrared network, which facilitates the user location, is a handicap in providing ubiquitous coverage [4]. However, they can only record how many people enter or exist in a restricted area by monitoring that area's access, such as the door of a room. Moreover, this technology requires careful and dense deployment, and does not work in a more complicated environment.

2.4 Pressure

An optional localization technology is to use acceleration and air pressure sensors to detect people's footsteps [15]. The obvious drawbacks of this technology are the high cost and need for careful deployment.

2.5 Ultrasound

The technologies using ultrasonic sensor networks usually require the target object to carry a transmitter or receiver. Most of them adopt an ultrasonic Time-Of-Flight (TOF) method to obtain location information or uses a combination of ultrasound and RF to provide a location-support service [13]. It allows applications running on mobile and static nodes to learn their physical locations by using listeners (receivers).

As mentioned earlier, three indoor localization models have been studied using the RF technology. They are 802.11, active RFID, and wireless sensor networks.

2.6 802.11

The technologies use a standard network adapter to measure signal strengths. They utilizes signal strength information from known multiple access points to locate objects. Usually a radio map of signal strength for each location [20] is built, and the target is required to carry a radio detector (receiver). Recently, there are also some works having no such requirement. For example, Device-free passive localization [3] well examined the feasibility of using radio signal dynamics for object detection with two pairs of 802.11 transceivers. No real deployment and experimental results were reported in this work. Its incremental work [24] focus on the detection function in a real environment, however, only tracking of single object is considered.

2.7 RFID

LANDMARC can localize the target object carrying an active RFID [10], [32]. It adopts a number of reference tags to alleviate the fluctuation feature in RSSI and then utilizes K nearest reference tags' coordinates to compute the coordinates of the tracking tag. This method also requires

1. In fact, we only take advantage of the communication behavior of sensor nodes, not the associated sensing device.

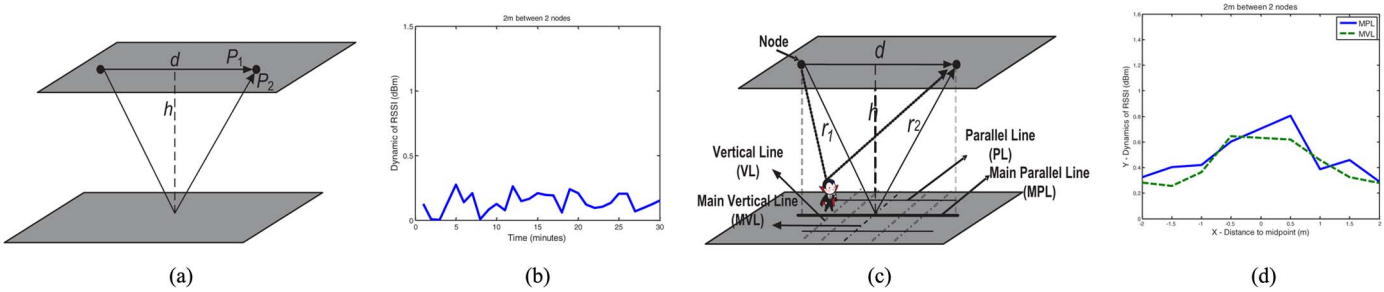

Fig. 1. Different environments vs. RSS dynamics caused by the target at different positions. (a) Static environment: there is no object moving around and all the environment factors remain unchanged. (b) Signal dynamics in the static environment, the distance between 2 nodes is 2 m. (c) Dynamic environment and position classification on the ground: at least one object moves in the environment. All other factors, such as temperature, remain unchanged. (d) Relationship between object distance and signal dynamics, when the distance between the 2 nodes is 2 m. The x axis is the target object distance to the midpoint of the 2 sensor nodes. The y axis is the signal dynamic.

the target object to carry a tracking tag (an active RFID). Tag-free [23] aims to find the object trajectory without carrying any device, by using data mining methods. Our work is very different from it. At first, their experiments are based on RFID [10] platform. Our work is based on sensor networks. Second, they leverage data mining methods, which require laborious training. Moreover, their work cannot get the trace of multiple objects.

2.8 UWB

Ultra narrow band adaptive tomographic radar is also a good technology able to detect transceiver-free object. However, since the communication range is limited for such technology, the cost is high in deployment.

2.9 Bluetooth

Many positional systems (e.g., [30]) leverage Bluetooth technology in localization. It requires a Bluetooth-capable handheld device carried by the target.

2.10 Accelerometer

There are a number of works using accelerometer signatures to help localization. For example, AAMPL [29] utilizes accelerometer signatures in mobile phones to correct locations derived from Google Maps. SurroundSense [28] uses not only the motion attributes from in-built accelerometers in phone, but also uses the optical, acoustic information from sensors to construct the fingerprint. In these work, the target object also has to carry a mobile phone (e.g., a Nokia N95 phone).

2.11 Wireless Sensor Networks

In RF-based WSNs, the information gathered from sensors is used to infer the global or application-defined local coordinates of the objects. Most of the object localization methods calculate distance or count the hop number to some nodes whose positions are already known, or measure the angle of arrival to derive location information [8], [9], [11], [21], [33]. Connectivity based algorithm [27] uses connectivity information to derive the location of nodes. For all these methods, the target object also has to carry a sensor node (transceiver) to send or receive the packets. ILight [25] tries to track moving object without carrying any device by using light sensors. However, this approach requires dense deployment and cannot work in dark area.

3 The Signal Dynamic Model

We have to understand how the movement of an object will affect the signal strength of two communicating sensor nodes. To focus on this effect, we consider a *static environment*, shown in Fig. 1a, where two sensor nodes are fixed on the ceiling with d distance apart and are h distance from the ground. For the corresponding *dynamic environment*, shown in Fig. 1c, at least one object moves in the environment. All other factors, such as temperature, remain unchanged.

3.1 Theoretical Background

In an indoor static environment, there should be two main radio propagation paths between the transmitter and the receiver besides the multi-path reflections of the surroundings. One is the line-of-sight path and the other is the ground reflection path as illustrated in Fig. 1a. When a finite-sized object comes into this static environment, as shown in Fig. 1c, it enters the dynamic environment. According to radar equation [12] and scattering theory [7], we may prove that the difference of signal strength between static environment and dynamic environment ΔP is approximately proportional to the following equation:

$$\Delta P = \frac{P_t G_t G_r \lambda^2 \sigma}{(4\pi)^3 r_1^2 r_2^2} \tag{1}$$

where r_1 and r_2 is the distance from the target object to the transmitter and the receiver, respectively. σ is the radar cross section of the target, which is 1 for human being [12]. The detail proof part is shown in the appendix.

3.2 Signal Dynamic Property

At first, we classify the object position on the ground as shown in Fig. 1c. The *main parallel line* (MPL) is the mapping on the ground of the transmitter-receiver. The *main vertical line* (MVL) is perpendicular to MPL crossing the midpoint of MPL. *Parallel Lines* (PL) and *Vertical Lines* (VL) are on the ground and parallel or equal to MPL and MVL, respectively. Second, suppose we have m number of RSSI values in the static environment, which are $a_1, a_2, \ldots, a_m$ and b is the RSSI

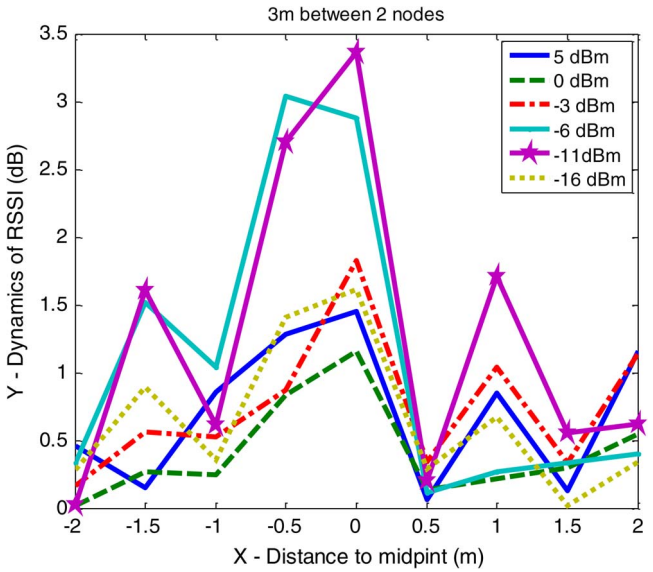

Fig. 2. Relationship between transmission power and signal dynamics.

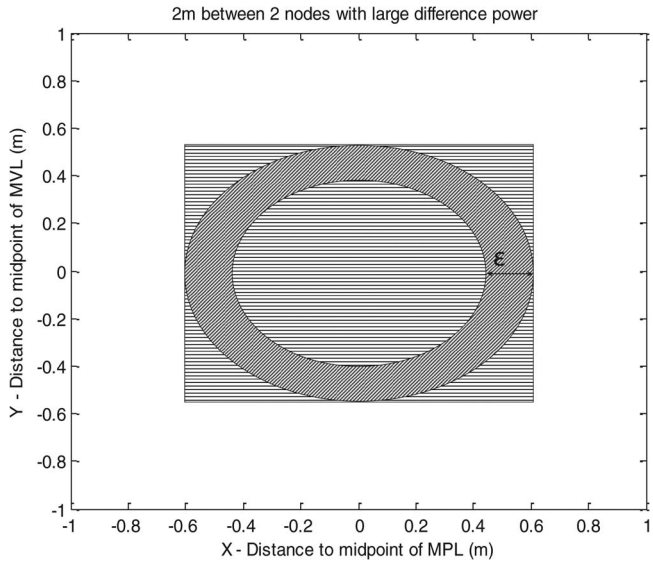

Fig. 3. Possible object area calculated by model.

value in the dynamic environment. We define the *RSSI dynamic* as below

$$\frac{\sum_{i=1}^{m} |b - a_i|}{m}.$$

Based on the theoretical background, we have the following property to describe the signal dynamics.

3.2.1 Signal Dynamic Property

Along each PL or VL, if the object position is closer to its midpoint, the RSSI dynamics caused by the object are larger.

The signal dynamic property is verified both in theory and experiments. The theory deduction and experimental verification are shown in the appendix. It is noted that, if in the static environment, where no object moves around, The RSSI dynamic is very small. One such example (the value of b is also from the static environment) is shown in Fig. 1b. We can see that the RSSI in static environment is relative stable.

We also conducted tests on the relationship between infrastructure node distance/transmission power and signal dynamics. Some examples are shown in Fig. 1d and Fig. 2. We found that the best side length between sensors in the grid is 2 m. The detail explanation and experiments are shown in the appendix. Moreover, there is a *sensitive transmission power* range that causes the biggest signal dynamics. By default, we use 0 dBm transmission power.

3.3 Estimation of the Possible Object Area

3.3.1 By Theory

From the signal dynamic properties introduced above, we may derive the possible object area on the ground, given a pair of nodes. According to Eq. (1), we may derive

$$r_1 r_2 = \sqrt{\frac{P_t G_t G_r \lambda^2 \sigma}{(4\pi)^3 \Delta P}} \tag{2}$$

here P_t is the transmitted power in watts, according to [12], $P_t = 0.001 * 2^{\text{dBm}/10}$, 0 dBm is corresponding to 1 mw. As introduced before, all the parameters above have fixed values for a fixed pair of nodes (assuming that one type of object is being localized). ΔP can also be calculated according to the RSSI data in the static environment and dynamic environment for the MICA2 nodes

$$\text{dBm} = (-50 * \text{RSSI} * 1.223/V) - 45.5 \tag{3}$$

where V is the battery voltage of the node.

We assume that for each pair of nodes and each time it receives data from which RSSI can be extracted, $r_1 r_2$ is a constant (i.e., objects' speeds are significantly less than the speed of light). As shown in Fig. 3, the possible object area in a perfect environment is on the border of an ellipse (projected to the ground). When ΔP is larger, $r_1 r_2$ is smaller, thus the ellipse is also smaller, and vice versa for smaller ΔP. Moreover, if we consider some error bound ε, the possible object area on the ground becomes a hollow ellipse as illustrated in Fig. 3. To describe this area more easily, we employ a bounding rectangle over the ellipse, and thus the area of the rectangle is an upper bound of the possible object area.

3.3.2 By Calibration

According to the theory introduced in the above section, we may use a bounding rectangle to represent the possible object area for a given signal dynamic value. In the real case, a more attractive option to obtain this area is by calibration manner.

Let L and W represent the length and width of the rectangle, respectively. Given a pair of nodes, to get the related value of L and W of the rectangle for a signal dynamic value, we perform the calibration for different node distances. For each node distance, we arrange a person to stand at different positions of its MPL and MVL, and then we record the related RSSI dynamic data. One of the calibration results on different link distances is shown in Fig. 4. For each link distance, no matter the object is on MPL or on MVL, the RSSI dynamics grow higher when the object moves closer to its midpoint.

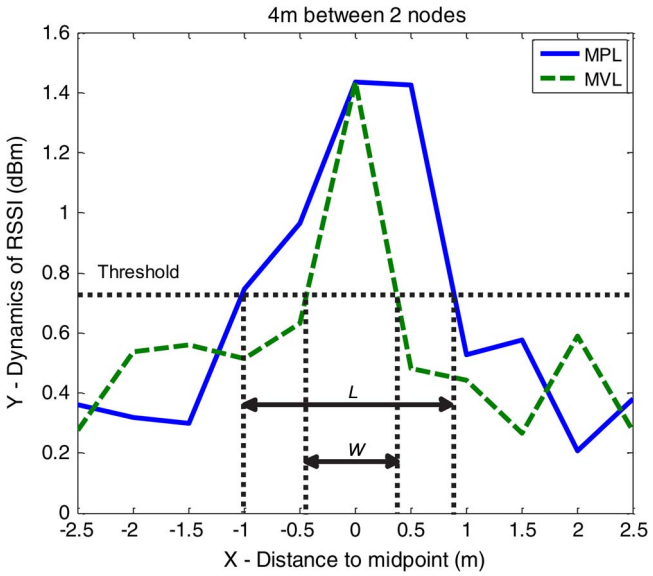

Fig. 4. Illustration of how to perform the calibration to get the possible object area based on one influential link.

After the calibration calculation we enter the calculation step. When we receive a signal dynamic value from this wireless link, we use this value to intercept the two lines, as shown in Fig. 4. We denote the interval on MPL as the length L of the rectangle, and the interval on MVL as the width W of the rectangle. Therefore, for different influential links with the different distances, we get the size of rectangles.

3.4 Probabilistic Signal Dynamic Model

Since the wireless signal behavior is very complex in real environment, it is more suitable to be modeled by probabilistic model.

3.4.1 Determine the Threshold

Since we leverage the signal dynamic values to determine the presence of the object and the object location, in practice, we should set a threshold to make this decision. At first, in the real case, to easily compare the signal dynamic value for different object locations, we use a normalized value of ΔP to represent, which is named ${}_{\Delta}P$

$$ {}_{\Delta}P = \frac{\Delta P(x,y) - \min(\Delta P(x,y))}{\max(\Delta P(x,y)) - \min(\Delta P(x,y))}. \quad (4) $$

Basically, we have to consider two kinds of errors. The first one is False Positive (FP) and the second one is False Negative (FN). Their definitions are as follows.

Definition. *False Positive (FP) is the probability that there is no target object in the field of interest (static environment), while the detection reports the presence.*

In the static environment, for a pair of nodes on the ceiling, we set their node distance as 3 m, the transmission power is 0 dBm. We sample 100 ΔP and normalize it into ${}_{\Delta}P$, and their Cumulative Distribution Function (CDF) is shown in Fig. 5a. We can see that, a small threshold of ΔP will introduce more FP and vice versa. For example, when the threshold is set to 0.2 (as the Threshold A in Fig. 8a), the value of FP is about $1 - 0.45 = 0.55$. But when the threshold is set higher to 0.5 (as the Threshold B in Fig. 8a), the value of FP is about $1 - 0.92 = 0.08$.

Definition. *False Negative (FN) is the probability that the target object is in the field of interest (dynamic environment), while the detection fails to report it.*

When the target is in presence, sometime the signal dynamic is not large enough to be detected, result in FN occurs. Based on the same node setting as test for FP, we choose different object locations (all measured as the distance to the midpoint on the ground). For each object location we sample 100 ΔP values and the CDF graph is shown in Fig. 5b. We can see that, different from FP, when we choose a higher threshold, the FN is larger, and vice versa. For example, if we choose the threshold as 0.3 (the Threshold C) in Fig. 5b, for the faraway target object (its distance to the midpoint on the ground is 10 m), the FP is about 0.46. While for the close object (the target on the midpoint on the ground), the FP is about 0.12.

If we want to lower down both FP and FN, the threshold should be set to minimize the summation of both FP and FN,

$$ {}_{\Delta}P_{th} = \arg\min_{{}_{\Delta}P} \big(FN({}_{\Delta}P) + FP({}_{\Delta}P) \big). \quad (5) $$

It should be noted that when the position of the target is different, the FN may vary. Fig. 5c shows Both FP and FN. For example, for the faraway object, the threshold should be set to 0.26. But for a nearby object, the threshold should be set to is 0.4. Therefore, in practice, the thresholds between 0.28 and 0.39 are suggested. We choose their average value 0.33 in our later experiment.

3.4.2 Discussion about the Threshold

In our first attempt to set this threshold, we usually choose the average signal dynamic values in the static environment. If this value is set too high, FN will grow higher, while if the value is set too low, FP will grow higher. Moreover, we find that, the target with different distance will cause different signal dynamics. If the target is far way, both FN and FP will grow higher, as shown in Fig. 5. Therefore, the threshold is sensitive to the distance of the target object. In practice, both far away objects and close objects may appear. Considering both the cases, we choose the threshold as the average ΔP value to both lower down the FP and FN value.

We also test different factors such as different indoor environments and different node distance. We find that, the FN and FP are not sensitive to different environments. But very larger node distance may affect the FP and FN. Due to the page limitation, we do not show figures. However, in our algorithms we skip those wireless links whose node distance is larger than 6 m (only use valid links). Therefore, our threshold does not consider this issue. More detail is shown in the appendix.

3.4.3 Detection Probability of the Estimated Possible Object Area

Since we conclude the threshold for the target object detection, in the dynamic environment, for each signal dynamic value we may detect the FN value from the FN

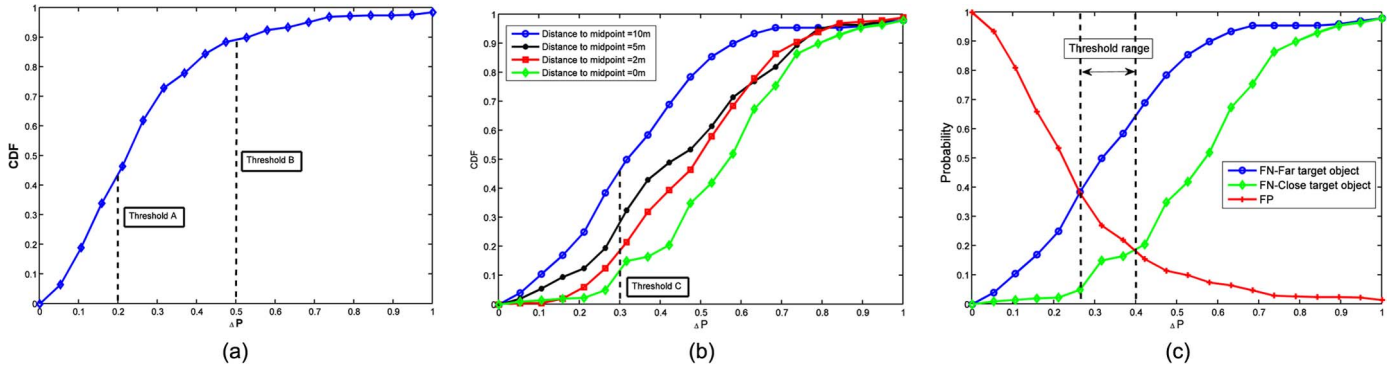

Fig. 5. Threshold setting decision. (a) CDF of ΔP in static environment. (b) CDF of ΔP in dynamic environment. (c) Threshold range to lower down both FP and FN.

figure. This FN value can be used to derive the detection probability of the estimated object location

$$\Pr_i = \Pr_i({}_{\Delta}P \geq {}_{\Delta}P_{th}). \tag{6}$$

Here $\Pr_i$ is the detection probability for the calculated object area of i-th wireless link. When ΔP is larger than the threshold given in the above subsection, the probability can be obtained from the FN figure of different wireless link. And we call such wireless links whose signal dynamic value larger than the threshold as *influential links*. Since the same ${}_{\Delta}P$ value may be resulted from different object locations. It may be far or may be nearby. Therefore, we choose the average value as the probability that the object in the detected area.

Therefore, we may conclude the probability the target object presents in the possible object area.

4 Methodology

Extending our signal dynamic model, we deploy sensors in a regular 2D grid array. The positions of all the nodes are predetermined. Each node acts as both transmitter and receiver. Our basic idea is to detect the RSSI dynamics caused by the objects. When the measured RSSI dynamics on a link is larger than the threshold, we call the link as an influential link (also defined in the last section). Based on the signal dynamic property, the influential links tend to cluster around the object. Thus, we can employ these influential links to locate the objects.

In this section, first we present 3 centralized algorithms to track single objects. Then, we present a distributed algorithm which is able to track multiple objects.

4.1 Centralized Algorithms

4.1.1 Midpoint Algorithm

Based on our model, by using the sensor grid, the influential links tend to cluster around the object. The midpoint algorithm utilizes the midpoints of the influential links to estimate the object location. We assign a weight value to the midpoint of each influential link according to its RSSI dynamic value. The object position can be calculated as the weighted average of these midpoints' positions.

Since the coordinates of all the sensor nodes are known in advance, for each influential link, the midpoint coordinate (x_i, y_i) can be calculated. The weight of each influential link is p_i, which is the RSSI dynamic value of the link. Assuming we have in total n influential links, we compute the weighted average of all the midpoints and get the object position coordinate value (x_{obj}, y_{obj}) as below

$$x_{obj} = \frac{\sum_{i=1}^{n} p_i \cdot x_i}{\sum_{i=1}^{n} p_i}, \quad y_{obj} = \frac{\sum_{i=1}^{n} p_i \cdot y_i}{\sum_{i=1}^{n} p_i}.$$

The complexity of the midpoint algorithm is $O(n)$, where n is the number of influential links.

4.1.2 Intersection Algorithm

The intersection algorithm improves the midpoint algorithm by using the intersection points of influential links instead of the midpoints of them. This is because more points on the influential links offer more information of the object location. If there are more intersection points, the possibility that the links are caused by noise is smaller. For each intersection point, we assign it a weigh value as the sum of RSSI dynamic values of the two crossing links. Then, we average all the intersection points to calculate the object position.

Suppose the number of influential links is n and the number of intersection points is l. We calculate the estimated object-position (x_{obj}, y_{obj}) as the weighted average value of all the intersection points

$$x_{obj} = \frac{\sum_{i=1}^{l} p_i \cdot x_i}{\sum_{i=1}^{l} p_i}, \quad y_{obj} = \frac{\sum_{i=1}^{l} p_i \cdot y_i}{\sum_{i=1}^{l} p_i}.$$

The total algorithm complexity is $O(n^2)$, where n is the number of influential links.

4.1.3 Best-Cover Algorithm

Instead of utilizing points on the influential links as described in previous algorithms, for each influential link, the best-cover algorithm creates a rectangle area, in which the object is likely to reside. The area of the rectangle is able to be calculated by our signal dynamic model. Therefore, in the sensor grid, there are many rectangles and some of them will overlap as shown in Fig. 6. It is obvious

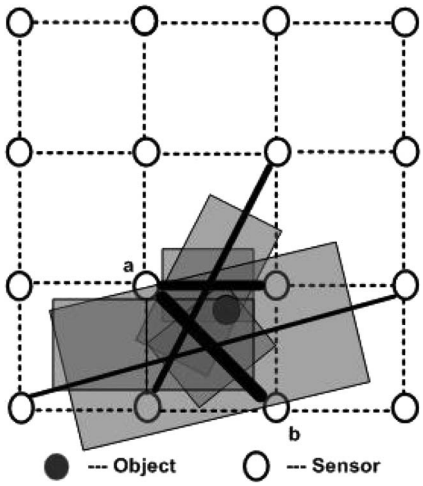

Fig. 6. Possible object area calculated by model.

that if one place has more overlapping rectangles, the object is more likely to be within that area. Therefore, in this algorithm, we use a square with a fixed area to scan in the grid area. At each scanning position, we calculate the sum of the intersection area between the scanning square and the generated rectangles on each influential link. We also define *covering rate* as the ratio of the number of rectangles intersecting with the scanning square to the total number of rectangles on all the influential links. The most possible object location is the position of the scanning square with the largest total covering area and the calculation reliability is according to its covering rate. Because the scanning square is an estimated area to represent the target object, such as a person, we adopt a square to be 0.5×0.5 square meters in our experiments.

Since we should compute the total covering area at each scanning-step and generate the rectangle for each influential link, the complexity of the best-cover algorithm is $O(nk)$, where n is the number of influential links and k is the total number of scanning times for the scanning square in the grid. The value of k depends on the side length of the grid array and the scanning step.

4.2 Distributed Algorithm

In this subsection, first we propose the *Distributed Dynamic Clustering* method to identify multiple objects. If multiple objects are not very close to each other, this algorithm can dynamically form different clusters for multiple objects. Also, instead of each node transmitting information on all these events back to the gateway for further processing, we use a distributed approach to identify the nodes located near each object and choose one node having the greatest remaining energy to be the cluster head. Each cluster head gathers local information about the signal dynamics of those influential links associated with those nodes within one hop. Then, we will employ the probabilistic cover algorithm at the cluster head pre-processing local information before sending the result back to gateway.

4.2.1 Distributed Dynamic Clustering (DDC)

This method aims at clustering the sensor nodes associated with the influential links, which are close to the objects.

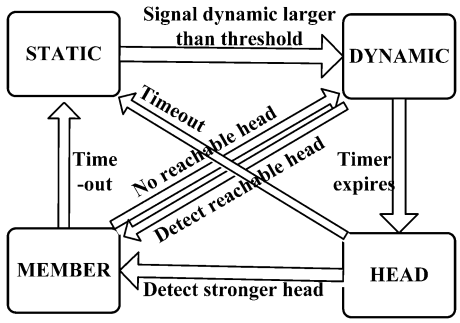

Fig. 7. Four states of event nodes in distributed dynamic clustering.

Multiple objects may cause multiple different clusters. This dynamic clustering mechanism is distinguished from other clustering work due to the short life time of clusters. The life time usually starts when influential links are detected and ends after the local information have been collected in the cluster head.

In DDC, each node has four states; the relationship of states is depicted in Fig. 7. At the beginning, all nodes are in the STATIC state. Each node builds a static table to store the static RSSI values for its neighbors after receiving beacons from neighbors. Nodes ignore packets transmitted from nodes beyond five meters (as explained in Section 3). The link thresholds are computed from these static RSSI values. When a node measures its received RSSI dynamic value larger than the threshold, it enters DYNAMIC state and starts an initial timer, signifying an *event detection*. The purpose of having an initial timer is to prevent more than one node in the next step from declaring themselves to be cluster heads at the same time (reducing communication overhead). The initial timer on node i at time t is defined in Equations (7) and (8)

$$t^i_{init(t)} = \left(1 - p^i_t\right) \times T_c + t_r \tag{7}$$

$$p^i_t = \frac{V^i_t - V_{\min}}{V_{\max} - V_{\min}}. \tag{8}$$

p^i_t is node i's remaining power described as the percentage over the node's initial power. We approximate the remaining energy by real-time voltage data which can be directly read from ADC readings in TinyOS. $V_{\max}$ is 3.0 V for a two AA battery powered sensor platform. T_c is a constant, which causes low energy nodes to wait at least T_c. T_c should be defined according to the transmission time of a single packet and the size of the cluster. In our experiments, we set T_c to half a second. t_r is a small random timer upper bound by T_c. By using this setting, we can force that the strongest node in each cluster will declare itself to be the cluster head.

During DYNAMIC state, the node will become a member node when it detects a reachable head. Otherwise, it will claim itself as a cluster head and enters the HEAD state after the timer expires. When a head node discovers a stronger head candidate within its reach (on hop away), it will transition into the MEMBER state and associate itself with the stronger head. If two nodes have the same remaining energy measure, node IDs will be used to break the tie. The head selection criteria will guarantee that the strongest node will be selected as the head. The head node

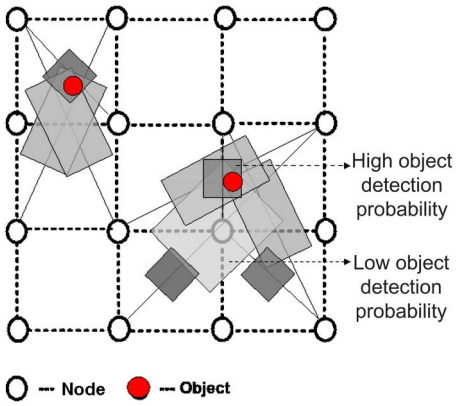

Fig. 8. Probabilistic cover algorithm.

also has the information of the influential links in its cluster. It should be noted that one MEMBER node can associate with more than one HEAD node. In other words, different clusters may incidentally overlap.

4.2.2 Probabilistic Cover Algorithm

After the head is chosen, it will use the signal dynamics information on the influential links from neighbors to estimate the object's position. The basic idea behind the probabilistic cover algorithm is to estimate a possible object area and the object detection probability of this area for each influential link, based on our probabilistic signal dynamic model. For each influential link i with a different distance, we can use the signal dynamic model to obtain the size of the rectangle and its object detection probability, according to our probabilistic signal dynamic model. As there may be many influential links, many such areas will be created. After estimating the possible object area on each influential link, in the node grid there will be many such rectangles as shown in Fig. 8. Rectangle i will have a detection probability Pr_i. Some of these rectangles will overlap. The object detection probability Pr_o of the overlapping area can be calculated as follows:

$$Pr_o = 1 - \prod(1 - Pr_i). \tag{9}$$

If one location has more rectangles with higher object detection probability, the object is more likely to be within that area. There may be several rectangle clusters in the area caused by either other objects or by noise. We ignore those clusters with small number of rectangles due to the high probability that they are caused by noise. The probabilistic cover algorithm is applied to each cluster. We use a fixed square area to scan in the cluster (to be described later). At each scanning step, we calculate the whole object detection probability of the rectangles that are intersecting with the square, and then select the position with the largest probability.

5 Performance Evaluation

In this section, we first describe our experimental setup and phases of the tracking system. Second, the investigation of dynamic threshold is given. Third, we compare the performance of the tracking algorithms proposed in the last section. Lastly, the tests of one moving object and multiple objects are provided.

5.1 Experimental Setup

We conduct our first experiments in an empty room with 12×9 square meters. Since the ceiling is not level, we hang the ropes from the ceiling to set up a 4×4 sensor grid. All the sensors are 2.40 meters above the floor. We use the popular MICA2 nodes with Chipcon CC1000 radio chips and monopole antennas [19]. Unless stated explicitly, the default transmission power is set as 0 dBm. The radio frequency is 870 MHz. We program all the sensor nodes to broadcast beacons periodically with the same interval. To avoid beacon collision, each node has to wait a short backoff time before broadcasting a beacon. The default beacon interval is three seconds.

5.2 Architecture of the Localization System

Generally, all the proposed tracking algorithms consist of two phases. First, in the initialization phase, each node builds a static table to store the static RSSI values for all its neighbors after receiving enough number of beacons. The link thresholds are also computed from those static RSSI values. The initialization phase has to be carried out in the static environment. After initializing all the nodes, the system enters the tracking phase. Each node measures the RSSI dynamic value to detect the influential links. If the RSSI dynamic value on a link is higher than the corresponding link threshold, the link is considered to be an influential link and the RSSI dynamic value is reported back to the sink node.

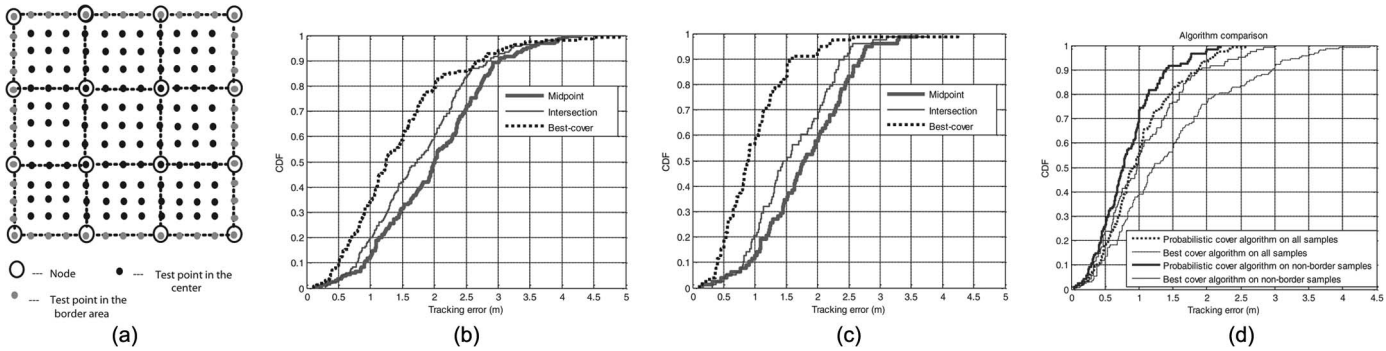

Fig. 9. Comparison of algorithms on a single object. (a) Test samples. (b) Comparison of centralized algorithms on all samples. (c) Comparison of centralized algorithms on non-border samples. (d) Comparison of best-cover algorithm and probabilistic-cover algorithm.

Otherwise, the dynamic value is used to update the static table.

5.3 Comparison of Algorithms on a Single Object

In our experiments, we test 169 sample positions in the area covered by the grid shown in Fig. 9a. Among these samples, 48 samples are on the border area of the grid.

For the 3 centralized algorithms, we find that the best-cover algorithm significantly outperforms the other two algorithms no matter for all the samples or for the non-border samples, as shown in Figs. 9b and 9c. Therefore, for the centralized algorithm, if high accuracy is not critical and with only one object, the intersection algorithm is a good choice as it is easy to implement and does not require calibration. Otherwise, the best-cover algorithm is recommended. We also compared the best-cover algorithm (perform the best in centralized algorithms) with the probabilistic algorithm. Based on the same tested samples, the average tracking error of each algorithm is shown in Fig. 9d. We find that the tracking error is improved by a factor of about 10percent for non-border samples, while for border samples this improvement can be greater than 20 percent. For non-border samples, the average tracking error can be reduced to 0.85 m. Fig. 10 shows one example of the object position estimated by probabilistic cover algorithm. In summary, the probabilistic cover algorithm provides a good improvement over the performance of the best cover algorithm, especially when target objects are on the border area.

5.4 The Effect of Multiple Objects

When there are multiple objects in the target area, as long as the objects are not tightly close to each other, the DDC method can easily separate them into different clusters. Within each cluster, the probabilistic cover algorithm is used to localize each object. In our experiments, we tested 20 different scenarios with two persons acting as moving objects. The average distance between the two persons is about 5 m. Experimental results show that in 18 out of the 20 cases we can differentiate between the two distinct objects, while the best cover algorithm can only differentiate them in 5 out of the 20 cases. The localization accuracy with DDC on average is 1.08 m. Fig. 11 shows a sample

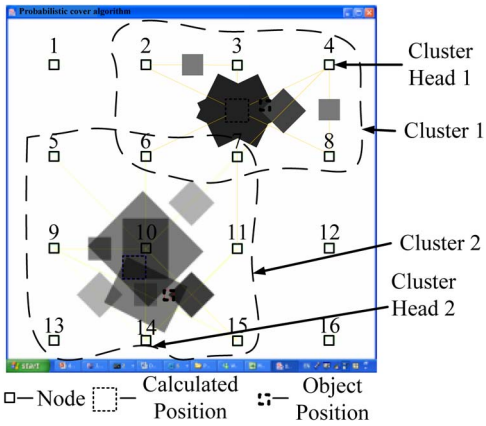

Fig. 11. Multiple object test 1.

example of the multiple object experiments. In this example, two clusters are formed by using DDC. It is worth mentioning that node 6 and node 7 belong to both clusters. They will send the received signal dynamics to both cluster heads. Fig. 12 is another example. We see two different clusters are formed. Compared to the localization accuracy 0.8 m of single object, the localization for multiple transceiver-objects is about 1 m. Their difference is only about 0.2 m. Therefore, probabilistic cover algorithm can localize multiple transceiver-free objects accurately.

5.5 Latency

When applying the centralized algorithm for tracking, the latency of detecting a person in the corresponding position is around $3s$, which is same as the time interval for sending beacon messages. When employing DDC method for tracking, we have two major types of delay. The first type of delay is the broadcast interval of beacons. Since there are contentions in the broadcast channel, the broadcast interval is determined by the density of the nodes and the transmission power of each node. As we reduced the transmission power of each node down to -10 dBm, the number of nodes within one cluster will be smaller. Therefore, we may reduce the time interval for sending beacon messages of each node to $1s$. Moreover, we could dynamically adjust the beacon intervals according to the signal dynamic it receives. If it is larger, the beacon interval is smaller, and

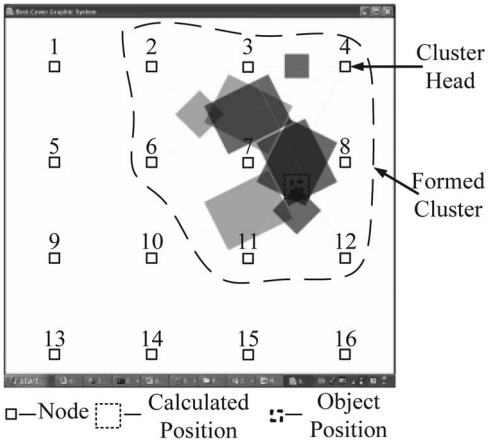

Fig. 10. Single object with the probabilistic-cover algorithm.

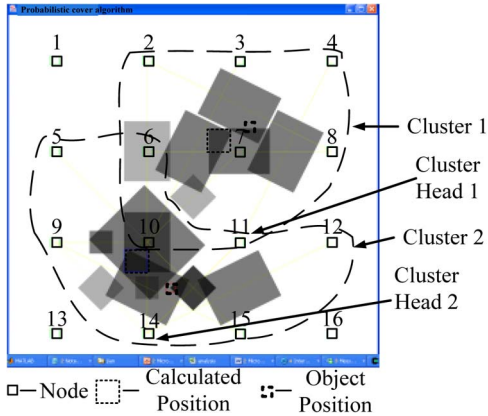

Fig. 12. Multiple object test 2.

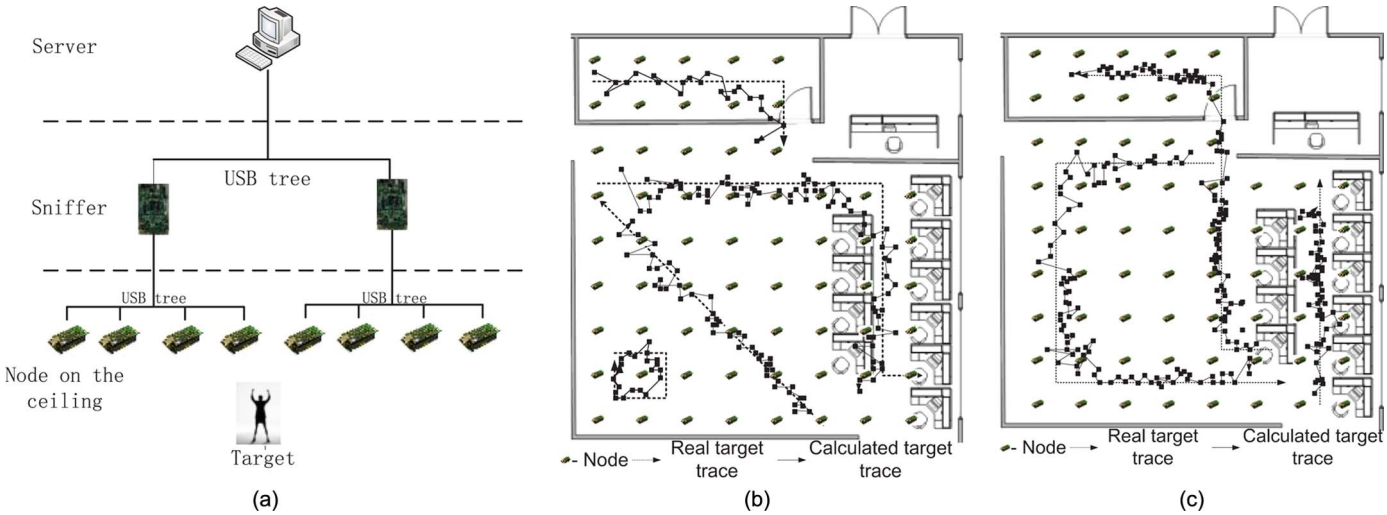

Fig. 13. Larger scale test. (a) System architecture. (b) Tracking 3 target objects. (c) Tracking 4 target objects.

vice versa. The second type of delay is the initial timer in the algorithm for turning a node from DYNAMIC state into HEAD state. As we described before, this value in our experiments is initially set around $0.5s$ and cannot be larger than 1 second.

To summarize, the probabilistic cover algorithms has smaller latency to totally about $2s$. The latency of the algorithm will not be sacrificed in large deployment.

5.6 Testing of Multiple Objects in a Larger Scale Set-Up Environment

We further tested our probabilistic cover algorithm with DDC method in a much larger indoor lab, which area is about 300 square meters. This area contains a big working place and a conference room, as shown in Figs. 13b and 13c. We deployed 63 TelosB sensors [19] with Chipcon *CC*2420. We bond each sensor by a paper belt and hang it on the ceiling. Each sensor is wired connected to the server by an USB tree. Our system is based on the Sensor Network Assistant Platform (SNAP) [31], which is also developed by our team. Our system connection architecture is shown in Fig. 13a. The reasons why we choose TelosB nodes instead of MICA2 nodes are as follows. First, they are much easier to be USB powered. Since there are many nodes to be deployed, wire setting can offer stable power supply. Furthermore, the RSS dynamic values of each wireless link and decentralized results of each sensor can be easily transmitted back to the sink, without wireless transmission delay. So it is able to better test our algorithms.

The TelosB nodes work on the radio frequency band from 2,400 to 2,483.5 MHz, and we verify their RSS dynamics behavior to the human being target obeys the our signal dynamic property. Further detail investigation of such feature is omitted due to the page limitation. Moreover, to reduce the interference among sensors, we lower down the transmission power to -10 dBm. The other setting is the same as our previous experiments. We arrange several people move around, and tested 50 target object traces. Two of them are shown in Figs. 13b and 13c. The First one shows the results when 4 people moving around. One person walked from the conference room to outside place. The latter one shows the results when 3 people walking around. One trace is along the aisle between the seats. The moving speed of each person is about 0.25 m/s. The dash lines are the real target traces, while the solid lines show the estimated target traces by using our probabilistic cover algorithm with DDC method. The average error is 0.94 m.

As result, our experiment shows that the probabilistic cover algorithm with DDC method is scalable in a larger area. As long as the target objects are not tightly close to each other, our algorithm may localize them accurately.

6 Conclusion and Future Work

This paper presented a signal dynamic model, three centralized algorithms and one distributed algorithm for tracking single and multiple transceiver-free objects in WSNs, respectively. It comprehensively analyzes tracking transceiver-free objects in an indoor environment using the RF-based technology. Our methods utilize the RSSI dynamic value between the static and the dynamic environment to calculate the target position. Among the three centralized algorithms, midpoint and intersection algorithms can be used for applications without requiring high accuracy. If some calibrations are performed in advance, the best-cover algorithm significantly beats the previous two. For the distributed algorithm, the intention of clustering tries to divide the events created by moving objects into clusters. In each cluster the probabilistic cover algorithm is used to calculate the object position. As long as the objects are not too tightly close to each other, the algorithm can differentiate between them. Moreover, the probabilistic cover algorithm can reduce the tracking latency. The small overhead of the proposed algorithm makes it more scalable for large deployment.

Furthermore, our system can also support moving object tracking. As long as the objects are not tightly close to each other, we can locate them. If the objects are tightly close to each other, we will recognize them as one object.

As future work, we will try other settings or irregular topologies to deploy sensors. Our approach to multiple moving objects still has some limitations when multiple objects cross each other's trajectory. We need to develop probabilistic models to analyze such dynamic behavior.

ACKNOWLEDGMENT

This research was supported in part by Hong Kong RGC Grant HKUST617811, by China NSFC Grants 61202377, 61170077, 61073180, 61170247, 61003272, 61103001, and 61272445, by Shenzhen Science and Technology Foundation under Grant JCYJ20120613173453717, and by China NSFGD Grant S2012040006682. Z. Ming and R. Mao are the corresponding authors.

REFERENCES

[1] D. Zhang, J. Ma, Q. Chen, and L.M. Ni, ''An RF-Based System for Tracking Transceiver-Free Objects,'' in *Proc. 5h Annu. IEEE Int. Conf. PERCOM*, 2007, pp. 135-144.
[2] D. Zhang and L.M. Ni, ''Dynamic Clustering for Tracking Multiple Transceiver-Free Objects,'' in *Proc. 7th Annu. IEEE Int. Conf. PERCOM*, 2009, pp. 1-8.
[3] M. Youssef, M. Mah, and A. Agrawala, ''Challenges: Device-Free Passive Localization for Wireless Environments,'' in *Proc. ACM 13th Annu. Int. Conf. MobiCom*, 2007, pp. 222-229.
[4] ACOREL Corporation, People Counting Technology using in Infrared, 1989. [Online]. Available: http://www.acorel.com
[5] Advanced Tracking Technologies, 2006. [Online]. Available: http://www.advantrack.com
[6] Q. Cai and J.K. Aggarwal, ''Automatic Tracking of Human Motion in Indoor Scenes Across Multiple Synchronized Video Streams,'' in *Proc. 6th Conf. IEEE Comput. Vis.*, 1998, pp. 356-362.
[7] J. Jackson, *Classical Electrodynamics,* 3rd ed. Hoboken, NJ, USA: Wiley, 1998.
[8] M. Maróti, P. Völgyesi, S. Dóra, B. Kusy, A. Nádas, Á. Lédeczi, G. Balogh, and K. Molnár, ''Radio Interferometric Geolocation,'' in *Proc. 3rd Int. Conf. Embedded Netw. Sens. Syst.*, 2005, pp. 1-12.
[9] S. Meguerdichian, S. Slijepcevic, V. Karayan, and M. Potkonjak, ''Localized Algorithms in Wireless Ad-Hoc Networks: Location Discovery and Sensor Exposure,'' in *Proc. 2nd ACM Int. Symp. Mobile Ad Hoc Netw. Comput.*, 2001, pp. 106-116.
[10] L.M. Ni, Y. Liu, Y.C. Lau, and A.P. Patil, ''LANDMARC: Indoor Location Sensing using Active RFID,'' in *Proc. 1st IEEE Int. Conf. PERCOM*, 2003, pp. 407-415.
[11] D. Niculescu and B. Nath, ''Ad Hoc Positioning System (APS) Using AOA,'' in *Proc. IEEE Conf. INFOCOM*, 2003, pp. 1734-1743.
[12] D. Pozar, *Microwave Engineering,* 2nd ed. Hoboken, NJ, USA: Wiley, 1998.
[13] N.B. Priyantha, A. Chakraborty, and H. Balakrishnan, ''The Cricket Location-Support System,'' in *Proc. 6th Annu. Int. Conf. MOBICOM*, 2000, pp. 32-43.
[14] T.S. Rappaport, *Wireless Communications: Principles and Practice* 2nd ed.,, Upper Saddle River, NJ, USA: Prentice-Hall, 2002.
[15] J.O. Robert and D.A. Gregory, ''The Smart Floor: A Mechanism for Natural User Identification and Tracking,'' in *Proc. CHI Conf. Human Factors Comput. Syst.*, 2000, pp. 275-276.
[16] A. Woo, T. Tong, and D. Culler, ''Taming the Underlying Challenges of Reliable Multihop Routing in Sensor Networks,'' in *Proc. 1st Int. Conf. Embedded Netw. SenSys*, 2003, pp. 14-27.
[17] G. Xu, *GPS: Theory, Algorithms and Applications.* Berlin, Germany: Springer-Verlag, 2003.
[18] D.B. Yang, H.H. Gonzalez-Banos, and L.J. Guibas, ''Counting People in Crowds with a Real-Time Network of Simple Image Sensors,'' in *Proc. 9th IEEE ICCV*, 2003, pp. 122-129.
[19] XBOW Corporation, XBOW MICA2/TelosB Mote Specifications. [Online]. Available: http://www.xbow.com
[20] J. Yin, Q. Yang, and L.M. Ni, ''Adaptive Temporal Radio Maps for Indoor Location Estimation,'' in *Proc. 3rd IEEE Int. Conf. PERCOM*, 2005, pp. 85-94.
[21] P. Zhang, C.M. Sadler, S.A. Lyon, and M. Martonosi, ''Hardware Design Experiences in ZebraNet,'' in *Proc. 2nd ACM Conf. Embedded Netw. SenSys*, 2004, pp. 227-238.
[22] R. Dorsch, G. Hausler, and J. Herrmann, ''Laser Triangulation: Fundamental Uncertainty in Distance Measurement,'' *Appl. Opt.*, vol. 33, no. 7, pp. 1306-1314, Mar. 1994.
[23] Y. Liu, L. Chen, J. Pei, Q. Chen, and Y. Zhao, ''Mining Frequent Trajectory Patterns for Activity Monitoring using Radio Frequency Tag Arrays,'' in *Proc. 5th Annu. IEEE Int. Conf. PERCOM*, 2007, pp. 2138-2149.
[24] M. Moussa and M. Youssef, ''Smart Cevices for Smart Environments: Device-Free Passive Detection in Real Environments,'' in *Proc. 7th Annu. IEEE Int. Conf. PERCOM*, 2009, pp. 1-6.
[25] X. Mao, S. Tang, X. Xu, X. Li, and H. Ma, ''iLight: Indoor Device-Free Passive Tracking using Wireless Sensor Networks,'' in *Proc. 30th IEEE INFOCOM*, 2011, pp. 281-285.
[26] TINYOS Alliance, TINYOS, 1999. [Online]. Available: http://www.tinyos.net
[27] Y. Shang, W. Ruml, Y. Zhang, and M. Fromherz, ''Localization From Connectivity in Sensor Networks,'' *IEEE Trans. Parallel Distrib. Syst.*, vol. 15, no. 11, pp. 961-974, Nov. 2004.
[28] M. Azizyan, I. Constandache, and R.R. Choudhury, ''SurroundSense: Mobile Phone Localization via Ambience Fingerprinting,'' in *Proc. 15th Annu. Int. Conf. MOBICOM*, 2009, pp. 261-272.
[29] A. OfstadRick, Szcodronski, and R.R. Choudhury, ''AAMPL: Accelerometer Augmented Mobile Phone Localization,'' in *Proc. ACM Workshops MELT*, 2008, pp. 13-18.
[30] S. Feldmann, K. Kyamakya, A. Zapater, and Z. Lue, ''An Indoor Bluetooth-Based Positioning System: Concept, Implementation and Experimental Evaluation,'' in *Proc. ICWN*, 2003, pp. 109-113.
[31] M. Gao, X. Pan, L. Deng, C. Huang, D. Zhang, and L. Ni, ''A Versatile Nodal Energy Consumption Monitoring Method for Wireless Sensor Network Testbed,'' in *Proc. 17th ICPDS*, 2011, pp. 388-395.
[32] Y. Zhao, Y. Liu, and L. Ni, ''VIRE: Virtual Reference Elimination for Active RFID-Based Localization,'' in *Proc. ICPP*, 2007, p. 56.
[33] N. Xia, H. Du, S. Li, R. Zheng, and R. Feng, ''VSPSA for Acoustic Source Localization in Wireless Sensor Networks,'' *Ad hoc Sens. Wireless Netw.*, vol. 19, no. 3/4, pp. 277-304, 2013.

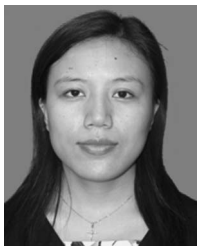

Dian Zhang received the PhD degree in computer science and engineering from the Hong Kong University of Science and Technology, Hong Kong, in 2010. After that, she worked as a Research Assistant Professor at Fok Ying Tung Graduate School, Hong Kong University of Science and Technology, Hong Kong. She is currently an Assistant Professor at Shenzhen University. Her research interests include wireless sensor networks, pervasive computing and networking and distributed systems. She is a member of the IEEE.

Kezhong Lu received the PhD degree in computer software and theory from the University of Science and Technology of China, China, in 2006. He is currently an Associate Professor at Shenzhen University. His research interests include wireless sensor networks and distributed computing. He is a member of the IEEE.

Rui Mao received the PhD degree in computer science from the University of Texas, Austin, TX, USA, in 2007. He joined Shenzhen University, China, in April 2010, and is now an Associate Professor. His research interests include big data indexing and parallel and distributed systems. He is a member of the IEEE.

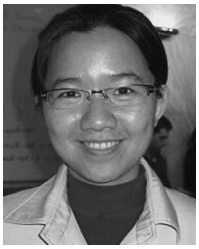

Yuhong Feng received the PhD in computer science from Nanyang Technological University. She is now an Associate Professor at Shenzhen University, China. Her areas of interest include distributed workflow management, grid and cloud computing, and Internet of things computing.

Yunhuai Liu received the PhD degree in computer science and engineering from the Hong Kong University of Science and Technology, Hong Kong. He is currently a Full Professor at the Third Research Institute of Ministry of Public Security. His research interests include wireless sensor networks, pervasive computing and Networking and Distributed Systems. He is a member of the IEEE.

Zhong Ming received the PhD in computer science from Zhong Shan University. He is now a Full Professor and Vice Dean at the College of Computer Science and Software Engineering, Shenzhen University, China. His areas of interest include software engineering, the Internet of things, distributed workflow management.

Lionel M. Ni received the PhD degree in electrical and computer engineering from Purdue University, West Lafayette, IN, USA, in 1980. He is Chair Professor and was Head of the Computer Science and Engineering Department at the Hong Kong University of Science and Technology. His research interests include parallel architectures, distributed systems, wireless sensor networks, high-speed networks and pervasive computing. As a Fellow of the IEEE, Dr. Ni has chaired many professional conferences and has received a number of awards for authoring outstanding papers.